

## ORIGINAL ARTICLE

# ADAP2 in heart development: a candidate gene for the occurrence of cardiovascular malformations in NF1 microdeletion syndrome

Marco Venturin,<sup>1</sup> Silvia Carra,<sup>2</sup> Germano Gaudenzi,<sup>2</sup> Silvia Brunelli,<sup>3</sup> Guido Roberto Gallo,<sup>2</sup> Silvia Moncini,<sup>1</sup> Franco Cotelli,<sup>2</sup> Paola Riva<sup>1</sup>

► Additional material is published online only. To view please visit the journal online (<http://dx.doi.org/10.1136/jmedgenet-2013-102240>).

<sup>1</sup>Dipartimento di Biotecnologie Mediche e Medicina Traslazionale, Università degli Studi di Milano, Milan, Italy

<sup>2</sup>Dipartimento di Bioscienze, Università degli Studi di Milano, Milan, Italy

<sup>3</sup>Dipartimento di Scienze della Salute, Università degli Studi di Milano-Bicocca, Monza (MB), Italy

**Correspondence to**

Dr Marco Venturin, Dipartimento di Biotecnologie Mediche e Medicina Traslazionale, Università degli Studi di Milano; Via Viotti 3/5, Milan 20133, Italy; marco.venturin@unimi.it

Dr Paola Riva, Dipartimento di Biotecnologie Mediche e Medicina Traslazionale, Università degli Studi di Milano; Via Viotti 3/5, Milan 20133, Italy; paola.riva@unimi.it

MV, SC, GG, FC and PR contributed equally to this study.

Received 19 December 2013

Revised 7 March 2014

Accepted 10 March 2014

**ABSTRACT**

**Background** Cardiovascular malformations have a higher incidence in patients with NF1 microdeletion syndrome compared to NF1 patients with intragenic mutation, presumably owing to haploinsufficiency of one or more genes included in the deletion interval and involved in heart development. In order to identify which genes could be responsible for cardiovascular malformations in the deleted patients, we carried out expression studies in mouse embryos and functional studies in zebrafish.

**Methods and results** The expression analysis of three candidate genes included in the NF1 deletion interval, *ADAP2*, *SUZ12* and *UTP6*, performed by in situ hybridisation, showed the expression of *ADAP2* murine ortholog in heart during fundamental phases of cardiac morphogenesis. In order to investigate the role of *ADAP2* in cardiac development, we performed loss-of-function experiments of zebrafish *ADAP2* ortholog, *adap2*, by injecting two different morpholino oligos (*adap2*-MO and UTR-*adap2*-MO). *adap2*-MOs-injected embryos (morphants) displayed in vivo circulatory and heart shape defects. The molecular characterisation of morphants with cardiac specific markers showed that the injection of *adap2*-MOs causes defects in heart jogging and looping. Additionally, morphological and molecular analysis of *adap2* morphants demonstrated that the loss of *adap2* function leads to defective valvulogenesis, suggesting a correlation between *ADAP2* haploinsufficiency and the occurrence of valve defects in NF1-microdeleted patients.

**Conclusions** Overall, our findings indicate that *ADAP2* has a role in heart development, and might be a reliable candidate gene for the occurrence of cardiovascular malformations in patients with NF1 microdeletion and, more generally, for the occurrence of a subset of congenital heart defects.

**INTRODUCTION**

NF1 microdeletion syndrome (MIM 613675) is a rare disorder caused by the haploinsufficiency of *NF1* and contiguous genes. NF1-microdeleted patients carry a heterozygous deletion of 17q11.2 region typically spanning about 1–1.4 Mb.<sup>1 2</sup> NF1 microdeletion syndrome is often characterised by a more severe phenotype compared to the one observed in NF1 with intragenic mutation.<sup>3</sup> Comparing the clinical phenotype between NF1-microdeleted patients and the whole NF1 population, we found that cardiovascular malformations (CVM) are significantly more

frequent in NF1 patients with microdeletion syndrome than in those with neurofibromatosis caused by intragenic mutation.<sup>4</sup> The CVMs found in the NF1-deleted patients include pulmonic stenosis, atrial/ventricular septal defects and valve defects, and show an incidence of 18% versus 2.1% displayed by NF1 patients with intragenic mutation.<sup>4 5</sup>

The higher incidence of CVMs in NF1-microdeleted patients is most likely dependent on the haploinsufficiency of genes lying in the deletion interval, presumably involved in heart morphogenesis. Our previous search for candidate genes by northern blotting and RT-PCR analysis evidenced that three genes encompassed by NF1 microdeletion, *SUZ12*, *ADAP2* (formerly *CENTA2*) and *UTP6* (formerly *C17ORF40*) are highly expressed in human fetal heart and during the early developmental stages of mouse embryonic heart,<sup>6</sup> thus deserving further analysis.

*SUZ12* (*Suppressor of Zeste 12 Homolog (Drosophila)*) is the human ortholog of the *Drosophila Su(z)12* polycomb gene, encoding a protein which is implicated in developmental mechanisms in *Drosophila*.<sup>7</sup> Mice lacking *Suz12* are not viable and die around 7.5 days post-coitum (dpc), displaying severe developmental and proliferative defects.<sup>8</sup>

*ADAP2* (*ArfGAP with Dual PH domains 2*) encodes a protein named Centaurin- $\alpha$ -2, which belongs to the centaurins protein family. Centaurin- $\alpha$ -2 is recruited to the plasma membrane where it specifically regulates actin cytoskeleton remodelling via ARF6, indicating an important role in exocytosis and cell motility.<sup>9</sup> Moreover, it was recently shown to interact with microtubules and to increase their stability.<sup>10</sup>

*UTP6* (*small subunit (SSU) processome component, homologue (yeast)*) is the human homologue of yeast *SSU processome component*. The *UTP6* gene is essential for efficient pre-rRNA processing<sup>11</sup> and seems to be involved in the positive regulation of apoptosis.<sup>12</sup>

Here, we investigated the spatio-temporal expression profile of *ADAP2*, *SUZ12* and *UTP6* murine orthologs during mouse embryonic and fetal development by in situ hybridisation. Based on this analysis, we held *ADAP2* the most interesting candidate gene for CVMs occurrence and used zebrafish as a model organism to investigate in vivo the role of *adap2*, the *ADAP2* zebrafish ortholog, during vertebrate heart development by loss-of-function experiments.

**To cite:** Venturin M, Carra S, Gaudenzi G, et al. *J Med Genet* Published Online First: [please include Day Month Year] doi:10.1136/jmedgenet-2013-102240

## RESULTS

**Expression analysis of *Suz12*, *Utp6* and *Adap2* genes in mouse reveals that *Adap2* is expressed during key stages of heart development**

In order to elucidate the expression pattern of *Suz12*, *Utp6* and *Adap2* genes in mouse, we performed in situ hybridisations using whole mounts at different stages of development, ranging from 7.5 to 11.5 dpc.

The gene which revealed the most interesting expression pattern was *Adap2*, since it was visible in heart between 9 and 10.5 dpc (figure 1) during fundamental phases of cardiac morphogenesis, namely heart looping (beginning at 8 dpc), endocardial cushion formation (10 dpc), and septation of the outflow tract, atria, and ventricles (10.5 dpc). In particular, the strongest *Adap2* mRNA hybridisation signal was seen in the heart atria and ventricles at 9.5 dpc (figure 1E), but its expression in the heart was visible as of 9 dpc (figure 1C) and was still present in the atria and ventricles at 10.5 dpc (figure 1F). We also performed in situ hybridisations on cryosections of 15.5 dpc embryos in order to assess if *Adap2* transcript is also present in the heart during the later stages of fetal cardiac development. Our experiments demonstrated that the expression of *Adap2* in the heart continues to be maintained at least until 15.5 dpc, in the ventricles and atria (figure 1H).

Conversely, *Suz12* evidenced a more spatially and temporally restricted expression in heart, with a clear hybridisation signal only at 10.5 dpc in the atrium, while *Utp6* revealed no expression in heart at any analysed stages (see online supplementary figure S1).

Based on this evidence, we held *ADAP2* the most interesting candidate gene for CVMs occurrence, and we used zebrafish as a model organism to investigate in vivo its role during vertebrate heart development.

***adap2*, the *ADAP2* zebrafish ortholog, is required for proper cardiac morphogenesis**

In order to explore the spatio-temporal expression pattern of *adap2*, the *ADAP2* zebrafish ortholog (Ensembl Gene ID: ENSDARG00000070565), we performed RT-PCR and whole-mount in situ hybridisation assays. *adap2* transcript was detected by RT-PCR at all analysed stages, from cleavage up to 120 hpf (hours post-fertilisation), as well as in the oocytes, indicating that the gene is maternally and zygotically expressed. Furthermore, *adap2* mRNA was present in all analysed adult tissues, including heart (see online supplementary figure S2). Whole-mount in situ hybridisation (WISH) revealed that *adap2* transcript was present in the heart at 2 dpf (days post-fertilisation) and 3 dpf stages, in the region corresponding to bulbus arteriosus (see online supplementary figure S2).

In order to investigate the potential role of *adap2* during zebrafish heart development in vivo, we performed loss-of-function experiments by injecting two independent translation-blocking morpholinos (*adap2*-MO and UTR-*adap2*-MO) which target the region surrounding *adap2* translation start codon and the 5'-UTR region, respectively. The injection of a control morpholino (std-MO) with no targets in zebrafish was used as control of the microinjection. At 2 dpf, most of embryos injected with 0.3 pmol of *adap2*-MO (morphants), unlike std-MO injected embryos, displayed blood circulation defects and curved tail (figure 2). Lower doses caused no circulatory defects. For the analysis of injected embryos, we focused our attention on 2 dpf, stage at which the circulation is surely started and the cardiac looping occurred in control embryos. At this stage, 61% (n=94)

of embryos injected with 0.3 pmol/embryo of *adap2*-MO showed one or more blood circulatory defects, such as the total loss of circulation (21%), accumulation of blood cells in the trunk and/or tail region (48%) and blood stases in the head (13%) (figure 2D–F,G). All these circulatory defects were noticed in both *adap2* morphants which showed a body axis comparable with that of control embryos and morphants which displayed a bent tail phenotype (71%, n=94). The injection of the second translation-blocking MO, UTR-*adap2*-MO, caused in vivo qualitatively similar defects to the first injected MO, though with a different penetrance (see online supplementary figure S3).

To rule out that circulation defects could be caused by alterations of vascular development, we carried out *adap2* loss-of-function experiments in the tg(*flk1*:EGFP) zebrafish transgenic line,<sup>13</sup> where EGFP expression is controlled by the endothelial-specific *flk1* promoter (see online supplementary figures S4 and S5). At 2 dpf, *adap2* knocked-down embryos revealed no gross defects in vascular development, with correct development of main axial vessels, dorsal aorta (DA) and cardinal vein (CV), indicating a normal vasculogenesis. Weak defects in intersomitic vessels (Se) were observed only in those embryos with a marked curved tail, suggesting that these alterations were likely caused by structural defects of body axis rather than by angiogenesis abnormalities.

The evidence that two independent morpholinos gave the same in vivo phenotypes confirmed the specificity of the *adap2* morpholinos. Consequently, we present here data obtained on embryos injected with the *adap2*-MO, which we indicate as *adap2* morphants.

The evidence that circulatory defects in *adap2* morphants were not caused by vascular defects suggested that they were most likely derived from an abnormal heart development and functionality. To test this hypothesis, we injected *adap2*-MO or std-MO in embryos belonging to the tg(*gata1*:dsRed)<sup>sd2</sup>;tg(*flk1*:EGFP)<sup>S84.3</sup> double transgenic line,<sup>14</sup> in which erythrocytes are labelled in red and endothelial cells are labelled in green; we observed the injected embryos under a confocal microscope (figure 3). At 2 dpf, control embryos displayed a normal heart morphology (figure 3A), while *adap2* morphants showed a reduction of atrioventricular (AV) canal bending, a partial lack of atrium and ventricle separation, as well as a reduced ventricle size (figure 3B,C). All analysed embryos displayed blood circulation.

The in vivo analysis of *adap2* phenotype in morphants prompted us to investigate their heart morphology by a molecular approach, through whole-mount in situ hybridisation assays with the cardiac-specific marker *cmlc2* (*cardiac myosin light chain 2*) (figure 4, see online supplementary tables S1 and S2). At 26 hpf, std-MO-injected embryos showed the linear cardiac tube correctly positioned ventrally in the left region of the embryo (left jog) (figure 4A). On the contrary, only 39% (n=59) of *adap2*-MO-injected embryos displayed, at the same stage, the correct leftward cardiac jogging (figure 4B), while another 39% showed no jog, with the heart tube situated centrally along the midline of the embryo (figure 4C). Finally, the remaining 22% of *adap2* morphants was characterised by an inverted cardiac jogging (right jog) (figure 4D). At 2 dpf, std-MO-injected embryos hybridised with the *cmlc2*-specific probe presented a normal S-shaped heart with the ventricle positioned on the right of the atrium, indicating a correct D-looping process (figure 4E). Differently, only 22% (n=49) of *adap2* morphants showed a heart morphology comparable to control embryos (figure 4F). The remaining *adap2*-injected

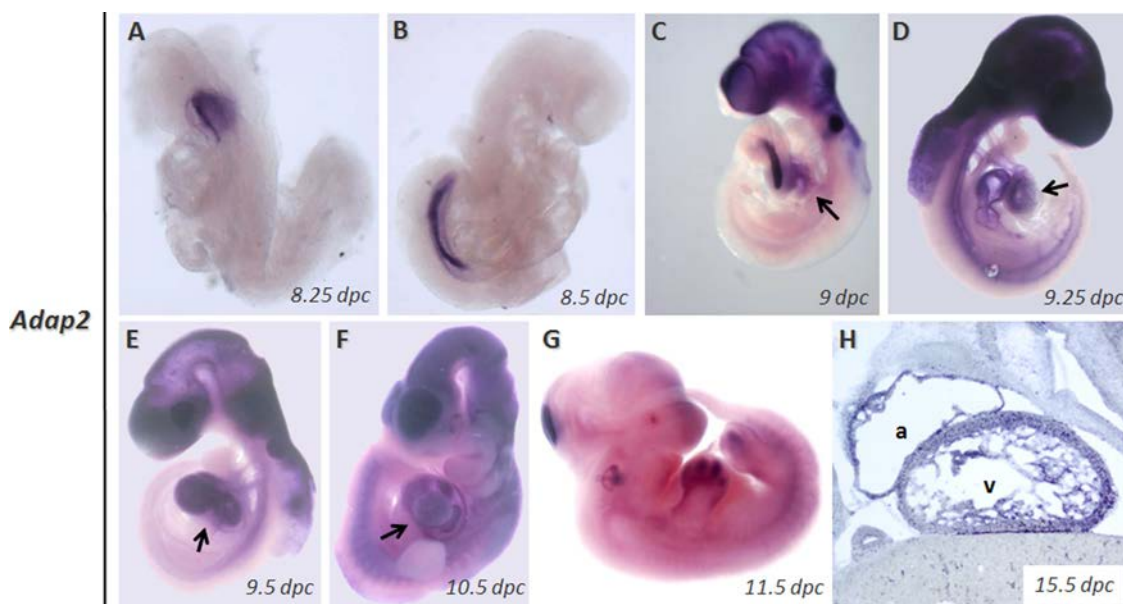


**Figure 1** Expression of *Adap2* in whole-mount mouse embryos and mouse cryosections. (A–G) Whole-mount in situ hybridisation on embryos from 8.25 dpc to 11.5 dpc with an *Adap2* specific probe. (A) 8.25 dpc, expression at the midbrain/hindbrain boundary. (B) 8.5 dpc, expression in the gut tube. (C) 9 dpc, expression in forebrain, midbrain, hindbrain, heart (arrow), otic vesicles, gut tube. (D) 9.25 dpc, expression in forebrain, midbrain, hindbrain, otic vesicles, heart (arrow), gut tube. (E) 9.5 dpc, expression in forebrain, midbrain, hindbrain, otic vesicles, heart (arrow), gut tube. (F) 10.5 dpc, expression in forebrain, midbrain, hindbrain, otic vesicles, heart (arrow), gut tube. (G) 11.5 dpc expression in midbrain, inner ear, forelimbs, weakly in hindlimbs. (H) In situ hybridisation on cryosection of a 15.5 dpc embryo showing *Adap2* expression in heart atrium (a) and ventricle (v).

embryos displayed either an intermediate phenotype with reduced looping (18%), or absence of looping with a completely linear heart tube (47%), or a reversed heart looping with the ventricle on the left of the atrium (12%) (figure 4G–I). Moreover, whole-mount in situ hybridisation assays with the ventricle-specific marker *vmhc* (*ventricular myosin heavy chain*) evidenced, at 2 dpf, a marked reduction of ventricle size in 64% (n=39) of *adap2* morphants, confirming the in vivo observations (see online supplementary figure S6). The reduction of ventricle size was observed regardless of the heart looping phenotype (D-loop, no loop or reversed loop). Notably, the percentage of embryos showing reduced ventricle size was similar in *adap2* morphants with or without blood circulation, 65% (n=29) and 60% (n=10) respectively, suggesting no relation between this defect and circulatory complications.

#### *adap2* loss-of-function affects AV valve development

In order to shed light on the effect of *adap2* knockdown on cardiac functionality, we analysed AV valve formation in zebrafish by carrying out histological sections of AV valve in *std*-MO and *adap2*-MO-injected embryos at different developmental stages. At 3 dpf stage, control embryos displayed correctly formed endocardial cushions in the AV canal connecting the two cardiac chambers (figure 5A). The *adap2* morphants morphologically more similar to *std*-MO-injected embryos still showed proper heart morphology with normal endocardial cushions, the only evident defect being a mild reduction of ventricle size, as already evidenced (figure 5B). In *adap2*-injected embryos which in vivo showed an intermediate phenotype (bent tail and presence of blood circulation), a visible alteration of the endocardial cushions was observed, with a marked disorganisation of the cellular elements that will be forming the mature AV valve (figure 5C). Embryos with severe phenotype, that is, curved tail and absent circulation, showed serious alterations in

the heart morphology, making impossible any consideration on endocardial cushion formation (figure 5D). The histological analysis of *std*-MO-injected embryos at 5 dpf evidenced a properly developed mature valve, recognisable as two flap-like structures in correspondence to the AV canal (figure 5E). At this stage, *adap2*-MO-injected embryos showing an in vivo mild phenotype were already characterised by evident defects of mature AV valve, whose cells resulted disorganised and poorly compact (figure 5F). The morphology of mature valves in morphants with curved phenotype and with blood circulation appeared more compromised, structurally disorganised, without the typical valvular shape and with cells irregularly disposed (figure 5G). Finally, the most affected *adap2* morphants showed severe cardiac malformations: the heart appeared essentially as a linear-shaped structure, without a clear separation between the two chambers, and consequently it was impossible to analyse mature cardiac valve conformation (figure 5H). Moreover, longitudinal histological sections of *adap2* morphants at 5 dpf evidenced an endocardial detachment from the myocardial layer notably in the atrial chamber (figure 5F,G).

To characterise at molecular level the cardiac AV valve defects displayed by embryos as a consequence of *adap2* functional inactivation, we analysed, by means of in situ hybridisation experiments, the expression pattern of two markers, *bmp4* (*bone morphogenetic protein 4*) and *notch1b* (*notch homolog 1b*), which at 2 dpf are specifically expressed within the myocardial and endocardial component of AV canal, respectively (figure 6A,E). At 2 dpf stage, 91% (n=46) of control embryos showed a *bmp4*-specific hybridisation signal precisely marking the myocardial component of AV canal, as expected (figure 6B). Differently, 51% (n=41) of *adap2*-MO-injected embryos displayed a disorganised and ectopically expanded *bmp4*-specific expression domain, notably as the ventricular chamber is concerned (figure 6C,D). These defects were observed in all the



## Genotype-phenotype correlations

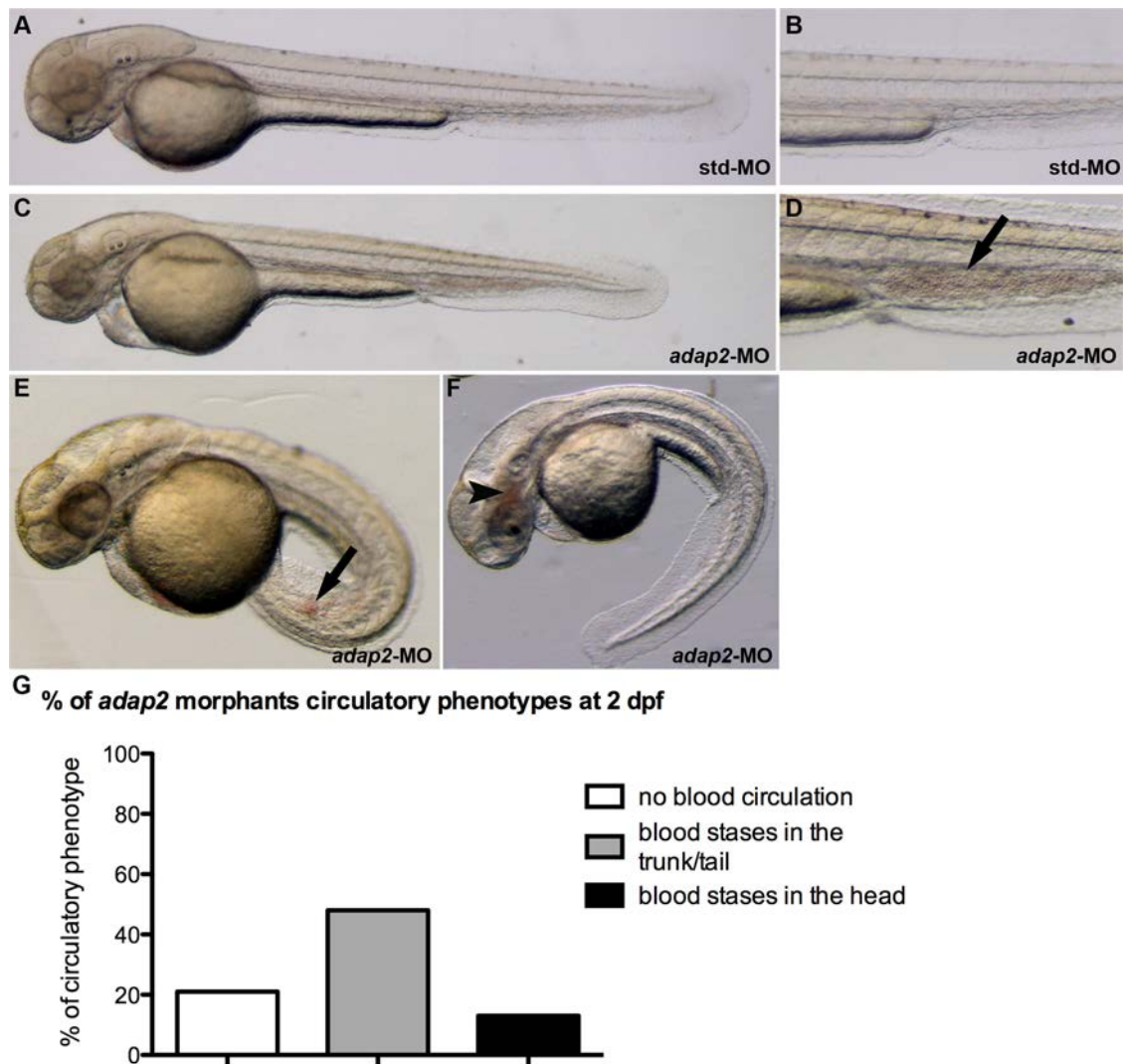


**Figure 2** *adap2* knockdown causes circulation defects in zebrafish. (A) Lateral view and (B) detailed image of the trunk-tail region of *std*-MO-injected embryos at 2 dpf. (C, E and F) Lateral view and (D) detailed image of the trunk-tail region of *adap2*-MO-injected embryos at 2 dpf. Anterior to the left. Black arrows: blood stases in the tail region; arrowhead: blood stasis in the head. (G) Percentage of circulation defects in *adap2* morphants at 2 dpf (n=94): 21% of the *adap2* morphants displayed no blood circulation, 48% blood stases in the trunk-tail region and 13% blood stases in the cephalic region.

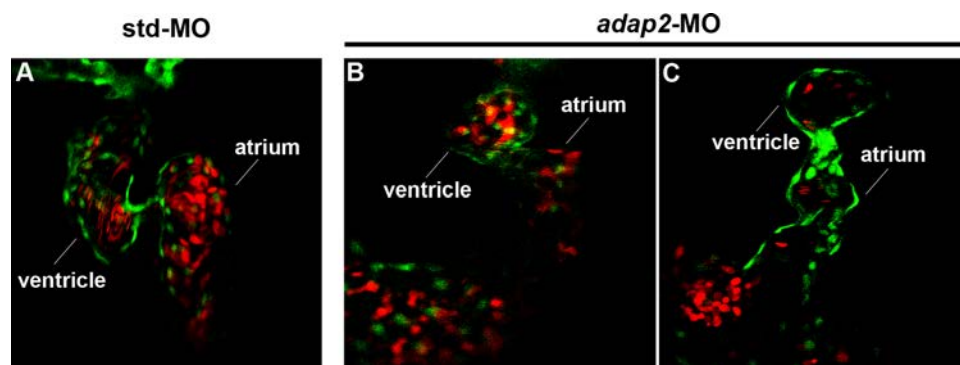


**Figure 3** *adap2* loss-of-function affects normal heart morphogenesis in zebrafish. The hearts of double transgenic  $tg(gata1:dsRed)^{sd2};tg(flk1:EGFP)^{S843}$  embryos injected with *std*-MO or *adap2*-MO were examined in vivo by confocal microscopy at 2 dpf. Erythrocytes and endocardium are labelled in red and green, respectively. Confocal images of the heart in (A) *std*-MO-injected embryo, in (B) *adap2* morphant displaying normal morphology and in (C) *adap2*-MO-injected embryo with bent tail. All analysed embryos presented blood circulation.

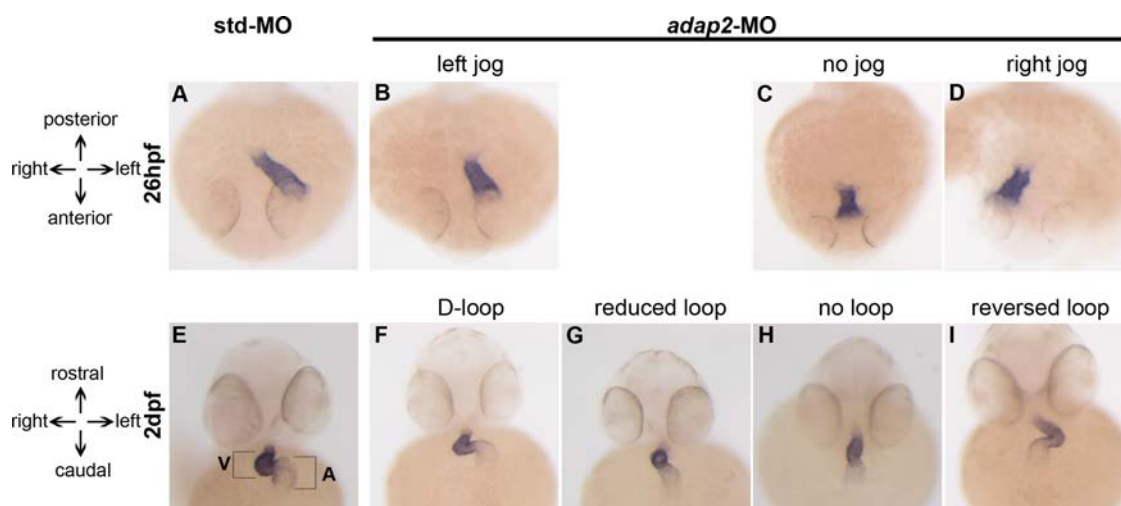


**Figure 4** *adap2* loss-of-function experiments perturb zebrafish heart jogging and heart looping. Analysis of *cmhc2* expression by in situ hybridisation was performed on *std-MO* and *adap2-MO*-injected embryos at 26 hpf and 2 dpf. The heart position in injected embryos was scored as left jog (normal; A and B), no jog (C) and right (reversed) jog (D) at 26 hpf and as D-loop (normal; E and F), reduced loop (G), no loop (H) and reversed loop (I) at 2 dpf. V: ventricle; A: atrium. (A–D) Dorsal views through the head, anterior to the bottom; (E–I) frontal views, head to the top.

phenotypic classes of heart development. Similar results were obtained from the analysis of *notch1b* marker at the same stage, with 49% (n=43) of *adap2-MO*-injected embryos displaying an expanded and disorganised *notch1b* expression pattern (figure 6G,H). All these data highlight *adap2* function in fundamental processes of zebrafish cardiac morphogenesis, notably heart jogging, heart looping, determination of ventricular size and AV valve formation.

Overall, our findings provide compelling evidence that *ADAP2* is involved in heart development, pointing to it as the most plausible candidate gene for the occurrence of congenital

CVMs in NF1 microdeletion syndrome and, more generally, for the occurrence of sporadic and familial congenital CVMs.

## DISCUSSION

Microdeletion syndromes are a group of disorders characterised by the deletion of a chromosomal segment spanning multiple disease genes, each potentially contributing to the phenotype independently. Microdeletion syndromes are often characterised by a complex clinical and behavioural phenotype resulting from the imbalance of normal dosage of genes located in that particular chromosomal segment.<sup>15</sup>

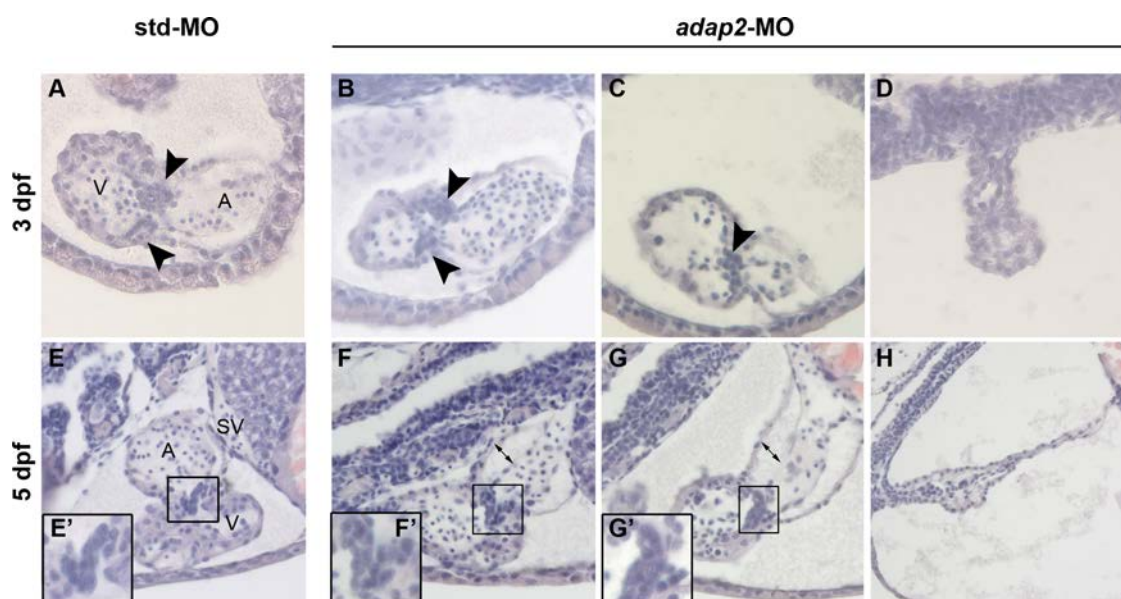


**Figure 5** *adap2* knockdown impairs the normal endocardial cushions and mature valve formation. Histological sections of *std-MO* and *adap2-MO*-injected embryos at 3 dpf (transversal sections) and 5 dpf (longitudinal sections) stained with haematoxylin and eosin. (A and E) Heart sections of control embryos at 3 dpf (A) and 5 dpf, with magnification of the valve region (E). (B and F) Heart sections of *adap2* morphants with blood circulation and morphology comparable to controls at 3 dpf (B) and 5 dpf, with magnification of the valve region (F). (C and G) Heart sections of *adap2* morphants with blood circulation and bent tail at 3 dpf (C) and 5 dpf, with magnification of the valve region (G). (D and H) Heart sections of *adap2* morphants with no blood circulation and curved tail at 3 dpf (D) and 5 dpf, with magnification of the valve region (H). Arrowheads: endocardial cushions; double arrows: extracellular matrix (cardiac jelly) located between myocardium and endocardium.

## Genotype-phenotype correlations

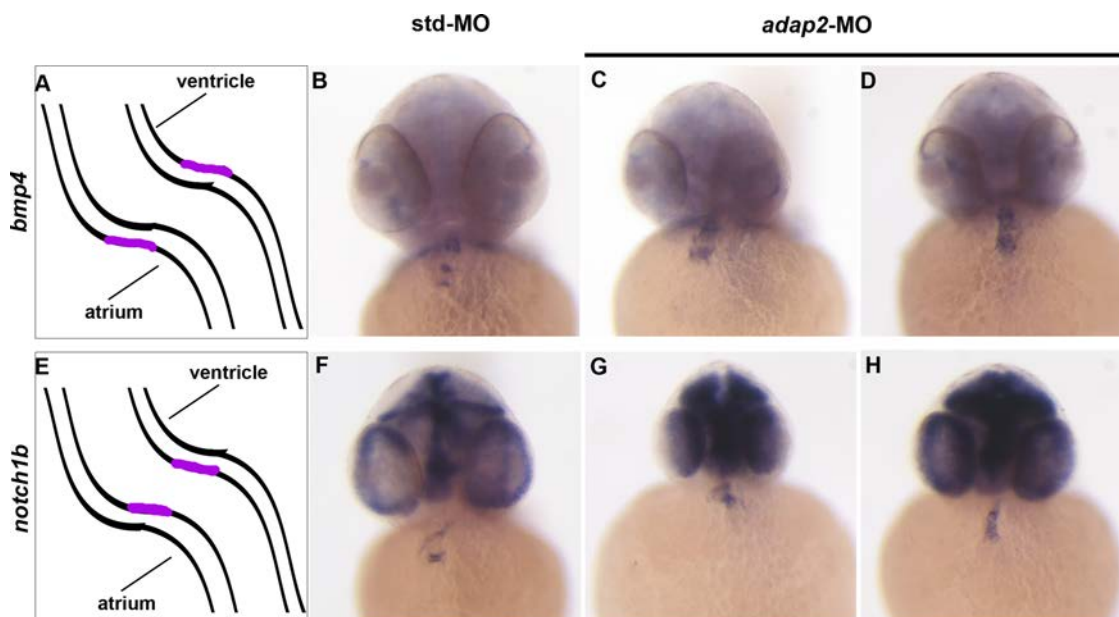


**Figure 6** The expression of atrio-ventricular boundary markers is affected in *adap2* morphants. The analysis of *bmp4* and *notch1b* expression by in situ hybridisation was performed on *std*-MO and *adap2*-MO injected embryos at 2 dpf. (A and E) Schematic representation of *bmp4* and *notch1b* expression domain in zebrafish heart at 2 dpf. The myocardium and endocardium-specific territories of *bmp4* and *notch1b* expression are depicted in magenta. (B and F) Embryos injected with *std*-MO displaying a normal hybridisation signal. (C, D and G, H) Embryos injected with *adap2*-MO displaying expanded and disorganised *bmp4* and *notch1b* expression domains. Frontal views are shown.

NF1 microdeletion syndrome is caused by heterozygous deletions involving the *NF1* gene and, in the most common 1.4 Mb deletion, other 14 genes.<sup>2</sup> A more severe clinical phenotype has often been reported in NF1 patients carrying the microdeletion compared to patients with intragenic *NF1* mutations.<sup>3</sup> By reviewing the phenotype of 92 patients with NF1 microdeletion, we found that CVMs occurred at a significantly higher incidence in this patient population as compared to NF1 patients with intragenic mutations,<sup>4</sup> suggesting that the whole-gene deletion segment encompasses important genes involved in heart development. Subsequent expression studies indicated three possible candidate genes for CVMs that warranted further studies: *ADAP2* (formerly known as *CENTA2*), *SUZ12* and *UTP6* (previously called *C17ORF40*).<sup>6</sup>

Here, we analysed the spatio-temporal expression profile of the above mentioned genes during mouse embryonic and fetal development. Based on this analysis, *Adap2* seems to be expressed in heart starting from 9 dpc, during key phases of cardiac development, that is when the heart tube is elongating and looping, and atrial and ventricular septa, as well as AV valves, are forming.<sup>16</sup> Moreover, *Adap2* expression in heart continues even in the later stages of development, at least until 15.5 dpc. Of note, *Adap2* expression is not restricted to a particular cardiac compartment or structure, but rather seems to localise in atria and ventricles. *Suz12* was also detected in heart during mouse development, but its expression seems to be restricted to a short period around 10.5 dpc and to the heart atria. Differently, *Utp6* showed no expression in the developing heart at all.

Since the expression of *ADAP2* mouse ortholog in heart during fundamental stages of cardiac morphogenesis was suggestive of a role in heart development, we studied the possible role of *ADAP2* in heart development by employing zebrafish as a model system. Over the recent years, zebrafish has proven to be a valid model for studying cardiovascular development. Despite its apparent simplicity, the zebrafish heart shares

common structural, developmental and genetics features with avian and mammalian heart.<sup>17–19</sup> Additionally, because of their small size, embryos receive enough oxygen by passive diffusion from external medium to survive and continue to develop in a relatively normal fashion for several days even in the complete absence of blood circulation, allowing a detailed phenotypic analysis of animals with severe cardiovascular defects that would be lethal in other organisms.<sup>20</sup>

The functional inactivation of *adap2*, the *ADAP2* zebrafish ortholog, obtained by the injection of two MO oligos targeting different *adap2* mRNA regions (translation start site and 5'-UTR), caused the same circulatory defects, proving the specificity of the phenotypes. We also designed a splice-blocking MO, which was predicted to cause exon 2 skipping, and to produce an altered form of *adap2* transcript with the generation of a premature stop codon. However, the injection of this MO at different doses did not cause any evident phenotypic defects. RT-PCR analysis, performed to test the efficacy of the splice-blocking MO, showed that only a fraction of *adap2* mRNA was incorrectly spliced. Consequently, we reason that the partial expression of the wild-type protein could be enough to prevent the occurrence of the phenotypic defects. This evidence, along with the presence in the embryo of the maternal transcript, which is targeted only by translation-blocking MOs, might explain the absence of alterations following the injection of this MO.

Our molecular results suggested *adap2* involvement in the cardiac jogging process, the morphogenetic process in which the heart cone is displaced to the left with respect to the anterior-posterior axis, which is one of the first evident breaks in left-right symmetry of the primitive zebrafish heart tube.<sup>21</sup> Moreover, *adap2* also appeared fundamental for the subsequent D-looping process, the bend of the heart tube to the right, which, by 36 hpf leads to the typical S-shaped heart, with the ventricle positioned on the right of the atrium. This was supported by the high number of *adap2* morphants, which at 2 dpf, when D-looping is normally completed, showed a linear heart,



a reduced loop or a reversed loop, all defects ascribable to alterations of the heart bending taking place during the D-looping process.

Functional inactivation of *adap2* also evidenced its important role during AV valve morphogenesis, since the earliest stages of endocardial cushion formation. Our results strongly suggest that a defective valvulogenesis results in impaired cardiac functionality, therefore, AV valve morphological alterations are most likely accounting for the in vivo blood circulation defects displayed by *adap2* morphants. Valve defects, including mitral valve prolapse, pulmonary valve stenosis and aortic valve anomalies, constitute a significant proportion of CVMs observed in patients with NF1 microdeletion syndrome.<sup>3 4</sup> Taking into account our findings on *ADAP2* role in valve morphogenesis, a correlation between *ADAP2* haploinsufficiency and the onset of valvular defects in NF1-microdeleted patients can be hypothesised. Additionally, the detachment between endocardium and myocardium observed in *adap2* morphants, particularly in the atrial chamber, could be caused by increased amounts of the extracellular matrix (cardiac jelly) juxtaposed between the two cardiac layers. Normal valve development involves multiple signalling pathways and extracellular matrix components take part in this process. Interestingly, dysregulation of components of the extracellular matrix seems to have a role in the myxomatous degeneration, the leaflet thickening and redundancy, typical of valvular abnormalities, such as mitral valve prolapse.<sup>22</sup>

*ADAP2* is known to regulate microtubule stability<sup>10</sup> and the activity of ARF6, a GTPase involved in cellular motility, adhesion and polarity by regulating cytoskeleton remodelling and cortical actin formation.<sup>9</sup> The alteration of these functions might impair adhesion and migration properties of AV valve cells, explaining their disorganisation and the irregular valve architecture observed in *adap2* morphants.

During the early phases of valve morphogenesis, the myocardial component of AV junction is fundamental for the signalling events leading endocardial cells to begin the formation of cushions, which will be later remodelled to create flap-like valvular structures.<sup>23</sup> The marked alteration of *bmp4* myocardial expression in *adap2* morphants suggests a compromised signalling from myocardium to endocardium, which might result in the structural valve defects observed at 5 dpf.

Overall, our study points to *ADAP2* as a gene involved in heart development, and as a plausible candidate gene for the occurrence of CVMs in NF1-microdeleted patients and in the general population, constituting an advance towards a better comprehension of the complex phenotypic spectrum of the syndrome, as well as of the genetic basis of CVMs.

## MATERIALS AND METHODS

### Animals

The mice used were of the CD1 strain (Charles River Laboratories International) and were housed in the pathogen-free facility at the San Raffaele Scientific Institute (Milano, Italy). Zebrafish (*Danio rerio*) embryos, collected by natural spawning, were raised and maintained according to established techniques.<sup>24</sup> Embryos were staged according to Kimmel and colleagues,<sup>25</sup> and raised at 28°C in fish water (Instant Ocean, 0.1% Methylene Blue) in Petri dishes. Beginning from 24 hpf, embryos were cultured in fish water containing 0.003% PTU (1-phenyl-2-thiourea; SIGMA) to prevent pigmentation. The following lines were used: AB (obtained from the Wilson lab, University College London, London, UK); *tg(flk1:EGFP)*<sup>13</sup> (from the Stainier lab, University of California at San Francisco, USA), *tg(gata1:dsRed)*<sup>sd2</sup>; *tg(flk1:EGFP)*S843<sup>14</sup> (from the

Santoro lab, Molecular Biotechnology Center, Università di Torino, Torino, Italy).

### RT-PCR

RT-PCR was performed on total RNA extracted from oocytes, embryos (about 30 embryos per sample) at different developmental stages and adult organs using the TOTALLY RNA isolation kit (Ambion), treated with RQ1 RNase-Free DNase (Promega) and oligo(dT)-reverse transcribed using Super-Script II RT (Invitrogen), according to the manufacturer's instructions. The following primers were used for PCR reactions: *adap2\_fw* 5'-GCTTAGACTTCTGGGATG-3', *adap2\_rev* 5'-CGAGATAACGGTTTTCAAGGC-3'. PCR products were loaded and resolved onto 2% agarose gels.

### In situ hybridisation

Probes were isolated by RT-PCR using specific primers (see online supplementary table S3) and cloned into the pCRII-TOPO vector (Invitrogen). Antisense and sense riboprobes were in vitro labelled with modified nucleotides (digoxigenin-UTP, Roche). WISH was performed on mouse embryos as described.<sup>26</sup> At least eight embryos per stage were analysed. Prehybridisation was performed in a formamide-tween20 solution, after which the DIG-labelled riboprobes were added to the embryos and incubated at 65°. In situ hybridisation on mouse cryostat sections was performed as described.<sup>27</sup>

WISH on zebrafish embryos was substantially carried out as described,<sup>28</sup> on embryos fixed for 2 h at room temperature in 4% paraformaldehyde/phosphate buffered saline, then rinsed with PBS-Tween, dehydrated in 100% methanol and stored at -20°C until processed for WISH.<sup>29</sup> A minimum of 20 embryos/time point were analysed.

The following probes were synthesised as described in the corresponding papers: *cmlc2* and *vmhc*,<sup>30</sup> *notch1b*<sup>31</sup> and *bmp4*.<sup>32</sup>

Images of stained embryos were taken with a Leica MZFLIII epifluorescence stereomicroscope equipped with a DFC 480 digital camera and IM50 Leica imaging software (Leica).

For histological sections, stained embryos were refixed in 4% paraformaldehyde, dehydrated, wax embedded, sectioned (8 µm) by a microtome (Leitz 1516) and stained with eosin. Images were taken with an Olympus BH2 microscope, equipped with a Leica DFC 320 digital camera and the IM50 software (Leica).

### Morpholino injections and phenotypic analysis

Antisense morpholinos (MOs; Gene Tools) were designed against the AUG translation start site region and the coding sequence, *adap2*-MO (5'-TTGTTCTTTTCCCGATTTGCCATAG-3') and against the 5'-UTR region, UTR-*adap2*-MO (5'-AAAACACTCCTGTGCGTCAGAATC-3'). As a control for unspecific effects, each experiment was performed in parallel with a std-MO (standard control oligo) with no target in zebrafish.

All morpholinos were diluted in Danieau solution<sup>33</sup> and injected at the 1–2-cells stage. Rhodamine dextran (Molecular Probes) was usually coinjected as a tracer. After injection, embryos were raised in fish water at 28°C and observed up to the stage of interest. For a better observation, the injected embryos were anaesthetised using 0.016% tricaine (Ethyl 3-aminobenzoate methanesulfonate salt, SIGMA) in fish water.

Images were acquired by using a Leica MZ FLIII epifluorescence microscope equipped with a Leica DCF 480 digital camera and the IM50 software (Leica). Confocal microscopy was performed with a Leica TCSNT confocal microscope equipped with an Ar/Kr laser (blocking filter BP 530/30 for EGFP and blocking filter LP 590 for ds Red).

## Genotype-phenotype correlations

For histological analysis 3 and 5 dpf zebrafish early larvae were fixed overnight at 4°C with bouin fixative. The samples were then dehydrated in a graded ethanol series, wax embedded, sectioned (8 µm) by a microtome (Leitz 1516) and stained with haematoxylin/eosin. Images were taken with a Leica DM6000 B microscope equipped with a Leica DCF480 digital camera and the LAS software.

**Acknowledgements** We thank U Fascio for his help in the acquisition of confocal images.

**Contributors** The study was conceived and designed by MV, SC, GG, PR, FC and SB. The experiments were carried out by MV, SC, GG, GRG and SM. The data were analysed by MV, SC, GG, PR, FC and SB. FC, PR and SB contributed reagents, materials and analysis tools. The paper was written and revised by MV, SC, GG, PR and FC.

**Funding** PR received an academic grant from Programma dell'Università per la Ricerca (PUR), University of Milan for this study.

**Competing interests** None.

**Provenance and peer review** Not commissioned; externally peer reviewed.

## REFERENCES

- Venturin M, Gervasini C, Orzan F, Bentivegna A, Corrado L, Colapietro P, Friso A, Tenconi R, Upadhyaya M, Larizza L, Riva P. Evidence for nonhomologous end joining and non allelic homologous recombination in atypical NF1 microdeletions. *Hum Genet* 2004;115:69–80.
- Pasmant E, Sabbagh A, Spurlock G, Laurendeau I, Grillo E, Hamel MJ, Martin L, Barbarot S, Leheup B, Rodriguez D, Lacombe D, Dollfus H, Pasquier L, Isidor B, Ferkal S, Soulier J, Sanson M, Dieux-Coeslier A, Bièche I, Parfait B, Vidaud M, Wolkenstein P, Upadhyaya M, Vidaud D. NF1 microdeletions in neurofibromatosis type 1: from genotype to phenotype. *Hum Mutat* 2010;31:E1506–18.
- Mautner VF, Kluwe L, Friedrich RE, Roehrl AC, Bammert S, Högel J, Spöri H, Cooper DN, Kehrer-Sawatzki H. Clinical characterisation of 29 neurofibromatosis type-1 patients with molecularly ascertained 1.4 Mb type-1 NF1 deletions. *J Med Genet* 2010;47:623–30.
- Venturin M, Guarnieri P, Natacci F, Stabile M, Tenconi R, Clementi M, Hernandez C, Thompson P, Upadhyaya M, Larizza L, Riva P. Mental retardation and cardiovascular malformations in NF1 microdeleted patients point to candidate genes in 17q11.2. *J Med Genet* 2004;41:35–41.
- Lin AE, Birch PH, Korf BR, Tenconi R, Niimura M, Poyhonen M, Armfield Uhas K, Sigorini M, Virdis R, Romano C, Bonioli E, Wolkenstein P, Pivnick EK, Lawrence M, Friedman JM. Cardiovascular malformations and other cardiovascular abnormalities in neurofibromatosis 1. *Am J Med Genet* 2000;95:108–17.
- Venturin M, Bentivegna A, Moroni R, Larizza L, Riva P. Evidence by expression analysis of candidate genes for congenital heart defects in the NF1 microdeletion interval. *Ann Hum Genet* 2005;69:508–16.
- Kuzmichev A, Nishioka K, Erdjument-Bromage H, Tempst P, Reinberg D. Histone methyltransferase activity associated with a human multiprotein complex containing the Enhancer of Zeste protein. *Genes Dev* 2002;16:2893–905.
- Pasini D, Bracken AP, Jensen MR, Lazzarini Denchi E, Helin K. Suz12 is essential for mouse development and for EZH2 histone methyltransferase activity. *EMBO J* 2004;23:4061–71.
- Venkateswarlu K, Brandom KG, Yun H. Pl-3-kinase-dependent membrane recruitment of centaurin-alpha2 is essential for its effect on ARF6-mediated actin cytoskeleton reorganisation. *J Cell Sci* 2007;120:792–801.
- Zuccotti P, Cartelli D, Stroppi M, Pandini V, Venturin M, Aliverti A, Battaglioli E, Cappelletti G, Riva P. Centaurin-a2 Interacts with b-Tubulin and Stabilizes Microtubules. *PLoS ONE* 2012;7:e52867.
- Champion EA, Lane BH, Jackrel ME, Regan L, Baserga SJ. A direct interaction between the Utp6 half-a-tetratricopeptide repeat domain and a specific peptide in Utp21 is essential for efficient pre-rRNA processing. *Mol Cell Biol* 2008;28:6547–56.
- Piddubnyak V, Rigou P, Michel L, Rain JC, Geneste O, Wolkenstein P, Vidaud D, Hickman JA, Mauviel A, Poyet JL. Positive regulation of apoptosis by HCA66, a new Apaf-1 interacting protein, and its putative role in the physiopathology of NF1 microdeletion syndrome patients. *Cell Death Differ* 2007;14:1222–33.
- Jin SW, Beis D, Mitchell T, Chen JN, Stainier DY. Cellular and molecular analyses of vascular tube and lumen formation in zebrafish. *Development* 2005;132:5199–209.
- Santoro MM, Samuel T, Mitchell T, Reed JC, Stainier DY. Birc2 (clap1) regulates endothelial cell integrity and blood vessel homeostasis. *Nat Genet* 2007;39:1397–402.
- Shaffer LG, Ledbetter DH, Lupski JR. Molecular cytogenetics of contiguous gene syndromes: Mechanisms and consequences. In: Scriver CR, Beaudet AL, Sly WS, Valle D, Childs B, Kinzler KW, Vogelstein B, eds. *The metabolic and molecular bases of inherited diseases*. New York: McGraw-Hill, 2001:6077–96.
- Savolainen SM, Foley JF, Elmore SA. Histology atlas of the developing mouse heart with emphasis on E11.5 to E18.5. *Toxicol Pathol* 2009;37:395–414.
- Weinstein BM, Fishman MC. Cardiovascular morphogenesis in zebrafish. *Cardiovas Res* 1996;31:E17–24.
- Stainier DY, Fouquet B, Chen JN, Warren KS, Weinstein BM, Meiler SE, Mohideen MA, Neuhaus SC, Solnica-Krezel L, Schier AF, Zwartkruis F, Stemple DL, Malicki J, Driever W, Fishman MC. Mutations affecting the formation and function of the cardiovascular system in the zebrafish embryo. *Development* 1996;123:285–92.
- Fishman MC, Stainier DY, Breitbart RE, Westerfield M. Zebrafish: Genetic and embryological methods in a transparent vertebrate embryo. *Meth Cell Biol* 1997;52:67–82.
- Stainier DY, Fishman MC. Patterning the zebrafish heart tube: acquisition of anteroposterior polarity. *Dev Biol* 1992;153:91–101.
- Chen JN, van Eeden FJ, Warren KS, Chin A, Nüsslein-Volhard C, Haffter P, Fishman MC. Left-right pattern of cardiac BMP4 may drive asymmetry of the heart in zebrafish. *Development* 1997;124:4373–82.
- Hayek E, Gring GN, Griffin BP. Mitral valve prolapse. *Lancet* 2005;365:507–18.
- Stainier DY. Zebrafish genetics and vertebrate heart formation. *Nat Rev Genet* 2001;2:39–48.
- Westerfield M. *The Zebrafish Book*. Eugene, OR: University of Oregon Press, 1993.
- Kimmel CB, Ballard WW, Kimmel SR, Ullmann B, Schilling TF. Stages of embryonic development of the zebrafish. *Dev Dyn* 1995;203:253–310.
- Avilion AA, Bell DM, Lovell-Badge R. Micro-capillary tube in situ hybridisation: a novel method for processing small individual samples. *Genesis* 2000;27:76–80.
- Strähle U, Blader P, Adam J, Ingham PW. A simple and efficient procedure for non-isotopic in situ hybridization to sectioned material. *Trends Genet* 1994;10:75–6.
- Thisse C, Thisse B, Schilling TF, Postlethwait JH. Structure of the zebrafish snail1 gene and its expression in wild-type, spadetail and no tail mutant embryos. *Development* 1993;119:1203–15.
- Jowett T, Lettice L. Whole-mount in situ hybridizations on zebrafish embryos using a mixture of digoxigenin- and fluorescein-labelled probes. *Trends Genet* 1994;10:73–4.
- Yelon D, Horne SA, Stainier DY. Restricted expression of cardiac myosin genes reveals regulated aspects of heart tube assembly in zebrafish. *Dev Biol* 1999;214:23–37.
- Westin J, Lardelli M. Three novel *Notch* genes in zebrafish: implications for vertebrate *Notch* gene evolution and function. *Dev Genes Evol* 1997;207:51–63.
- Nikaido M, Tada M, Saji T, Ueno N. Conservation of BMP signaling in zebrafish mesoderm patterning. *Mech Dev* 1997;61:75–88.
- Nasevicus A, Ekker SC. Effective targeted gene 'knockdown' in zebrafish. *Nat Genet* 2000;26:216–20.





## **ADAP2 in heart development: a candidate gene for the occurrence of cardiovascular malformations in NF1 microdeletion syndrome**

Marco Venturin, Silvia Carra, Germano Gaudenzi, et al.

*J Med Genet* published online April 7, 2014  
doi: 10.1136/jmedgenet-2013-102240

---

Updated information and services can be found at:  
<http://jmg.bmj.com/content/early/2014/04/07/jmedgenet-2013-102240.full.html>

---

	<i>These include:</i>
<b>Data Supplement</b>	"Supplementary Data" <a href="http://jmg.bmj.com/content/suppl/2014/04/07/jmedgenet-2013-102240.DC1.html">http://jmg.bmj.com/content/suppl/2014/04/07/jmedgenet-2013-102240.DC1.html</a>
<b>References</b>	This article cites 31 articles, 12 of which can be accessed free at: <a href="http://jmg.bmj.com/content/early/2014/04/07/jmedgenet-2013-102240.full.html#ref-list-1">http://jmg.bmj.com/content/early/2014/04/07/jmedgenet-2013-102240.full.html#ref-list-1</a>
<b>P&lt;P</b>	Published online April 7, 2014 in advance of the print journal.
<b>Email alerting service</b>	Receive free email alerts when new articles cite this article. Sign up in the box at the top right corner of the online article.

---

Advance online articles have been peer reviewed, accepted for publication, edited and typeset, but have not yet appeared in the paper journal. Advance online articles are citable and establish publication priority; they are indexed by PubMed from initial publication. Citations to Advance online articles must include the digital object identifier (DOIs) and date of initial publication.

---

To request permissions go to:  
<http://group.bmj.com/group/rights-licensing/permissions>

To order reprints go to:  
<http://journals.bmj.com/cgi/reprintform>

To subscribe to BMJ go to:  
<http://group.bmj.com/subscribe/>

**Topic  
Collections**

Articles on similar topics can be found in the following collections

[Reproductive medicine](#) (485 articles)  
[Genetic screening / counselling](#) (787 articles)  
[Congenital heart disease](#) (76 articles)  
[Molecular genetics](#) (1155 articles)

---

**Notes**

---

Advance online articles have been peer reviewed, accepted for publication, edited and typeset, but have not yet appeared in the paper journal. Advance online articles are citable and establish publication priority; they are indexed by PubMed from initial publication. Citations to Advance online articles must include the digital object identifier (DOIs) and date of initial publication.

---

To request permissions go to:

<http://group.bmj.com/group/rights-licensing/permissions>

To order reprints go to:

<http://journals.bmj.com/cgi/reprintform>

To subscribe to BMJ go to:

<http://group.bmj.com/subscribe/>